PCCP

ROYAL SOCIETY OF CHEMISTRY

PAPER

View Article Online
View Journal | View Issue

Cite this: *Phys. Chem. Chem. Phys.*, 2024, **26**, 24809

Dynamical electron correlation and the chemical bond. III. Covalent bonds in the A_2 molecules (A = C–F)†

Thom H. Dunning Jr. * and Lu T. Xu

Received 24th April 2024,
Accepted 16th September 2024

DOI: 10.1039/d4cp01695e

rsc.li/pccp

For most molecules the spin-coupled generalized valence bond (SCGVB) wavefunction accounts for the effects of non-dynamical electron correlation. The remaining errors in the prediction of molecular properties and the outcomes of molecular processes are then solely due to dynamical electron correlation. In this article we extend our previous studies of the effects of dynamical electron correlation on the potential energy curves and spectroscopic constants of the AH and AF (A = B–F) molecules to the homonuclear diatomic molecules, A_2 (A = C–F). At large R the magnitude of $\Delta E_{DEC}(R)$, the correlation energy of the molecule relative to that in the atoms, increases nearly exponentially with decreasing R, just as we found in the AH and AF molecules. But, as R continues to decrease the rate of increase in the magnitude of $\Delta E_{DEC}(R)$ slows, eventually leading to a minimum for C_2–O_2. Examination of the SCGVB wavefunction for the N_2 molecule around the minimum in $\Delta E_{DEC}(R)$ did not reveal a clear cause for this puzzling behavior. As before, the changes in $\Delta E_{DEC}(R)$ around R_e were found to have an uneven effect on the spectroscopic constants of the A_2 molecules.

Introduction

The reliable prediction of molecular properties and the outcomes of molecular processes requires an explicit consideration of electron correlation. Since electron correlation is traditionally defined relative to the restricted Hartree–Fock (RHF) wavefunction,[1] Sinanoğlu[2] noted that there were two distinct contributions to electron correlation. The first contribution is that due to the interaction of the RHF configuration with close-lying electronic configurations. These near degeneracies arise in an atom because of the degeneracies that arise as $Z \rightarrow \infty$, *e.g.*, the near degeneracy of the $2s^2$ and $2p^2$ configurations in beryllium-like atoms,[3,4] or they arise in molecules as $R \rightarrow \infty$, *e.g.*, the near degeneracy of the $1\sigma_g^2$ and $1\sigma_u^2$ configurations in H_2.[5] The second contribution is due to the instantaneous interactions among the electrons, which imposes challenging constraints on the electronic wavefunction, *e.g.*, when r_{ij}, the distance between any two electrons, approaches zero.[6,7] The latter type of correlation poses the greatest computational challenge for electronic structure calculations and is the least understood. These two types of correlation are commonly referred to as non-dynamical and dynamical electron correlation, respectively.

For most molecules, including the molecules considered in the current study, the spin-coupled generalized valence bond (SCGVB) wavefunction[8] includes the configurations that account for all the effects of non-dynamical correlation. The SCGVB wavefunction describes the dissociation of a molecule into its atomic fragments and includes the non-dynamical near-degeneracy effects in the atoms. Thus, the errors in the predictions from SCGVB theory are solely due to dynamical electron correlation. The clear demarcation between non-dynamical and dynamical electron correlation provided by the SCGVB wavefunction offers an opportunity to obtain a more thorough understanding of the effect of dynamical electron correlation on a broad range of molecular properties and processes as well as providing insights into the basic nature of dynamical electron correlation.

Two recent articles in this journal have proposed definitions for non-dynamical and dynamical electron correlation[9,10] that do not depend on the definition of a wavefunction, such as the SCGVB wavefunction, to describe non-dynamical electron correlation. These alternate definitions of the two types of electron correlation are valuable because, in a molecule, the nature of the configurations defining non-dynamical electron correlation may change as a function of the internuclear distance. For example, in the H_2 molecule at $R = \infty$, the $1\sigma_u^2$ configuration clearly represents a non-dynamical correlation effect. However, as $R \rightarrow 0$, the $1\sigma_u^2$ configuration of the H_2 molecule becomes the $2p\sigma^2$ configuration of the helium atom, which represents a

Department of Chemistry, University of Washington, Seattle, Washington 98195, USA. E-mail: thdjr@uw.edu

† Electronic supplementary information (ESI) available. See DOI: https://doi.org/10.1039/d4cp01695e

dynamical correlation effect. These changes raise two related questions:

• How does the contribution of the $1\sigma_u^2$ configuration to non-dynamical and dynamical correlation change as a function of R?

• Does the contribution of the $1\sigma_u^2$ configuration switch from non-dynamical to dynamical correlation only very close to the united atom limit or does it extend to distances approaching R_e.

Application of the above definitions of non-dynamical and dynamical correlation to H_2 as well as the other molecules that we have studied would add additional insights into the basic nature of non-dynamical and dynamical correlation in molecules.

In two previous studies,[11,12] we examined the effect of dynamical electron correlation on the spectroscopic constants and potential energy curves of the ground states of the AH and AF molecules (A = B–F), which have covalent bonds, and the first excited states of CH and CF, which have recoupled pair bonds.[13] At large internuclear distances, R, we found that the magnitude of the dynamical correlation energy increased nearly exponentially for all molecules, with a slight curvature for the AF molecules. At shorter distances, however, there were significant variations in the dynamical correlation energy, which led to irregular changes in the major spectroscopic constants, (R_e, ω_e, D_e). The resulting changes in the potential energy curves and spectroscopic constants could be correlated with changes in the orbitals and/or spin couplings in the SCGVB wavefunction. In this article we extend our earlier studies to examine the effect of dynamical electron correlation on the potential energy curves and spectroscopic constants of the homonuclear diatomic molecules, A_2 (A = C–F).

The results reported in our previous studies[11,12] as well as here are, in spirit, closely related to the earlier studies of Mok *et al.*[14] with two major exceptions:

• These authors used valence CASSCF (vCAS) wavefunctions[15] to define the non-dynamical correlation energy. Although the vCAS wavefunction includes all the configurations in the SCGVB wavefunction,[8] it also includes additional configurations that represent dynamical correlation.

• These authors used a combination of theoretical and experimental data to determine the total correlation energy and its dependence on the internuclear distance. Here we use the results from a correlated multireference wavefunction to determine the total correlation energy.

Our work is also related to that of Sears and Sherrill.[16] These authors explored how the choice of multiconfiguration reference wavefunction affected the ability of the corresponding calculations to recover the non-dynamical correlation energy and concluded that a set of configurations similar or equivalent to those in the SCGVB wavefunction efficiently and effectively captured non-dynamical correlation effects.

Theoretical and computational considerations

The SCGVB wavefunction can take many forms depending on the constraints imposed on the orbitals. It can be constructed with N orbitals for N electrons, as a Restricted Hartree–Fock (RHF) wavefunction, or as a wavefunction between these two extremes.[17–19] One of the most efficient and effective forms of the SCGVB wavefunction is one that describes the dissociation of a molecule into its constituent atoms as described by RHF theory plus any atomic near-degeneracy configurations. The basic form of this wavefunction is:

$$\Psi_{\mathrm{SCGVB}} = \hat{a}\varphi_{\mathrm{c1}}\varphi_{\mathrm{c1}}\cdots\varphi_{\mathrm{cn_c}}\varphi_{\mathrm{vn_c}}\varphi_{\mathrm{v1}}\varphi_{\mathrm{v1}}\cdots\varphi_{\mathrm{vn_v}}\varphi_{\mathrm{vn_v}}\phi_{\mathrm{a1}}\cdots\phi_{\mathrm{an_a}} \alpha\beta\ldots\alpha\beta\alpha\beta\ldots\alpha\beta\Theta^{n_a}_{S,M_S} \quad (1)$$

In eqn (1), $\{\phi_{ci}\}$ and $\{\phi_{vi}\}$ refers to the doubly occupied core and valence orbitals of which there are $n_c + n_v$, $\{\varphi_{ai}\}$ to the singly occupied active valence orbitals of which there are n_a, and $\Theta^{n_a}_{S,M_S}$ to an n_a-electron spin function for a state of total spin S and spin projection M_S appropriate for the n_a electrons in the active orbitals. All orbitals in the SCGVB wavefunction, both doubly and singly occupied orbitals, as well as the spin function, $\Theta^{n_a}_{S,M_S}$, are variationally optimized at each geometry. Although this form of the SCGVB wavefunction corresponds to a traditional covalent valence bond wavefunction, as noted by Coulson and Fischer[5] and discussed in more detail by Wilson,[20] optimization of the orbitals incorporates the effects of ionic configurations in the SCGVB wavefunction.

Although the orbitals in eqn (1) are fully optimized, in most molecules the resulting molecular orbitals are semi-localized and resemble hybrid orbitals, bond orbitals, lone pair orbitals, *etc.* in line with traditional valence bond concepts. The lone pair orbitals are largely localized on one atom with only small "tails" on other atoms. The bond orbitals are also largely localized on one of the atoms involved in the bond but have a significant "tail" on the atoms to which they are bonded. It is this "tail" that leads to the incorporation of ionic character into the SCGVB wavefunction.[5,20] Because the atomic origins of the SCGVB orbitals are usually well defined, we often use the atomic orbital designations followed by a prime to identify them. For example, in the N_2 molecule, the singly occupied bond orbitals in N_2, using N_A and N_B to represent the two atoms, are the $N_A2p\sigma'$, $N_B2p\sigma'$, $N_A2p\pi'_x$, $N_B2p\pi'_x$, $N_A2p\pi'_y$ and $N_B2p\pi'_y$ orbitals and the doubly occupied lone pair orbitals are the N_A2s' and N_B2s' orbitals. As $R \rightarrow \infty$, these orbitals become the singly occupied N2pσ, N2pπ_x, and N2pπ_y and doubly occupied N2s RHF orbitals of the two nitrogen atoms. The primes serve to indicate that, although the orbitals resemble the atomic orbitals, they have been optimized at each value of the internuclear distance R and are not simply atomic orbitals.

The spin function in eqn (1) is a linear combination of all the linearly independent ways to couple the spins of the electrons to obtain a state of total spin S and spin projection M_S:[21]

$$\Theta^{n_a}_{S,M_S} = \sum_{k=1}^{f_S^{n_a}} c_{S,k}\Theta^{n_a}_{S,M_S;k} \quad (2)$$

where $f_S^{n_a}$ is the number of linearly independent spin coupling modes. Optimization of the spin function, *i.e.*, the $\{c_{S,k}\}$

coefficients in eqn (2), enables the SCGVB wavefunction to smoothly describe the transition from the spin coupling appropriate for the separated atoms to that appropriate for the molecule. For example, for the N_2 molecule the dominate spin function at R_e has the spins of the electrons in the bond pairs, ($N_A2p\sigma'$, $N_B2p\sigma'$), ($N_A2p\pi'_x$, $N_B2p\pi'_x$), and ($N_A2p\pi'_y$, $N_B2p\pi'_y$), singlet coupled, whereas at $R = \infty$ the spins of the electrons in the (N2pσ, N2pπ_x, N2pπ_y) orbitals on each atom are coupled into a quartet and then the two quartets are coupled to give a singlet state. Optimization of $\Theta^{n_a}_{S,M_S}$ enables this transition to be continuously and smoothly described. Various spin bases, *e.g.*, Kotani, Rumer and Serber, can be used for the spin couplings in $\left\{\Theta^{n_a}_{S,M_S;k}\right\}$. The various spin bases offer different insights into the electronic structure of the molecule, although each spin basis leads to the same SCGVB wavefunction; see ref. 21 for more details.

The SCGVB wavefunctions for C_2, N_2 and F_2 are of the form given in eqn (1) and provide excellent zero-order descriptions of the molecules at all internuclear distances of interest. Although there is no atomic near-degeneracy effect in the ground states of the N_2–F_2 molecules, this is not the case in C_2 where the C $2s^2 \rightarrow 2p^2$ configuration makes a notable contribution to the atomic and molecular wavefunctions.[22] Both the SCGVB and vCAS wavefunctions include the configurations that account for this near-degeneracy effect. At R_e, the spin functions for the N_2 and F_2 molecules, $\Theta^{n_a}_{S,M_S}$, are dominated by three and one singlet-coupled electron pairs, respectively. As shown by Xu and Dunning[23] this is not the case for C_2 (see also ref. 24). Nonetheless, C_2 is still well described by the SCGVB wavefunction (far better than the RHF wavefunction; see ref. 23 for a direct comparison).

For O_2, a projected SCGVB wavefunction is required to obtain a wavefunction with the proper Σ^- symmetry. The projected SCGVB wavefunction consists of two SCGVB configurations, each with four singly occupied orbitals and associated spin functions:

$$(O_A1s')^2(O_B1s')^2(O_A2s')^2(O_B2s')^2(O_A2p\sigma')(O_B2p\sigma')\left(O_A2p\pi'_x\right)^2 \left(O_B2p\pi'_x\right)\left(O_A2p\pi'_y\right)\left(O_B2p\pi'_y\right)^2$$

$$(O_A1s')^2(O_B1s')^2(O_A2s')^2(O_B2s')^2(O_A2p\sigma')(O_B2p\sigma')\left(O_A2p\pi'_x\right) \left(O_B2p\pi'_x\right)^2\left(O_A2p\pi'_y\right)^2\left(O_B2p\pi'_y\right)$$

The projected SCGVB calculations on the $X^3\Sigma^-$ state of the O_2 molecule were performed using the "n_a-electrons in m_a-orbitals" SCGVB, SCGVB(n_a, m_a), method developed by Karadakov *et al.*[25] The spin function for the SCGVB wavefunction for O_2 at R_e is dominated by a singlet-coupled ($O_A2p\sigma'$, $O_B2p\sigma'$) pair and a triplet-coupled (O2pπ'_x, O2pπ'_y) pair.

To compute the dynamical electron correlation energy, a wavefunction that provides the exact electronic energy of a molecule is necessary. Although the treatment of non-dynamical correlation energy requires only a finite number of configurations as noted above, the calculation of the dynamical correlation energy formally requires an infinite number of configurations. To obtain a suitable proxy for the dynamical electron correlation energy, we used a vCAS wavefunction plus all single and double excitations (vCASCI).[26] A vCASCI calculation scales as N^6 where N is related to the number of atoms and electrons in the molecule. Although this scaling limits the applicability of the vCASCI method to modest size molecules, vCASCI calculations are possible for all the molecules considered here.

The vCAS wavefunction for the C_2 molecule is well behaved at all R. However, this is often not the case when the 2s orbitals make only a minor contribution to the vCAS wavefunction.[27] To prevent any undue mixing of the 1s and 2s orbitals as a function of the internuclear distance, R, in the N_2–F_2 molecules, we kept both the 1s and 2s orbitals doubly occupied in an initial vCAS calculation. We then froze the core orbitals from this vCAS calculation and re-optimized the full vCAS wavefunction. Finally, we carried out the vCASCI calculations, correlating all the electrons in the valence space.

All calculations used the aug-cc-pVQZ basis sets for the atoms.[28,29] These basis sets are sufficiently close to the complete basis set limit that they are expected to yield accurate SCGVB energies as well as reasonably accurate vCASCI energies (see later discussion). All calculations presented in this study were performed with the Molpro suite of quantum chemical programs (version 2010.1, 2023.2).[30,31] The CASVB module in Molpro was used to perform the SCGVB calculations[32,33] with Kotani spin functions. The standard settings provided by Molpro for convergence, *etc.* were used in all calculations reported here.

Results and discussion

With the definitions given in the last section, the dynamical electron correlation energy as a function of the internuclear distance, R, is simply:

$$E_{DEC}(R) = E_{vCASCI}(R) - E_{SCGVB}(R) \quad (3a)$$

In addition to $E_{DEC}(R)$, we are also interested in the differential dynamical correlation energy, *i.e.*, the change in $E_{DEC}(R)$ relative to its value at $R = \infty$:

$$\Delta E_{DEC}(R) = E_{DEC}(R) - E_{DEC}(\infty) \quad (3b)$$

as well as the equilibrium geometry-shifted differential dynamical correlation energy:

$$\Delta E_{DEC}(\Delta R) = E_{DEC}(\Delta R) - E_{DEC}(\infty) \quad (3c)$$

with $\Delta R = R - R_e$. $\Delta E_{DEC}(\Delta R)$ defines $\Delta E_{DEC}(R)$ with respect to the R_e for each molecule. For both the SCGVB and vCASCI calculations, the value of $E_{DEC}(\infty)$ in eqn (3b) and (3c) was taken to be the energies at the largest value of R considered (R = 20.0 Å). In all cases, the smallest values of R considered corresponded to energies above that of the separated atoms, *i.e.*, the values of R considered here fully covered the bound portion of the potential energy curves.

In the following section we examine the impact of dynamical electron correlation on the spectroscopic constants, (R_e, ω_e, D_e), of the A_2 molecules (A = C–F). As we shall see, the effect depends on both the magnitude and shape of $\Delta E_{DEC}(R)$ at or around R_e. We then report and discuss the impact of dynamical electron correlation on the potential energy curve of the C_2 molecule. Unlike the other molecules considered here, interaction between two low-lying C_2 states, the $X^1\Sigma_g^+$ and $B'^1\Sigma_g^+$ states, has a significant impact on $E_{DCE}(R)$. In the following section we report and discuss the effect of dynamical electron correlation on the potential energy curves of the N_2–F_2 molecules. We found minima in the $\Delta E_{DEC}(R)$ curves for C_2–O_2 as well as a visible increase in the $\Delta E_{DEC}(R)$ curve for F_2, although no minimum was found for the range of R considered. In the last section we examine the SCGVB wavefunction for N_2 in the vicinity of the minimum in $\Delta E_{DEC}(R)$ to investigate the underlying cause of the minima.

Spectroscopic constants of the A_2 molecules

The total energies at the calculated equilibrium bond distance, E_e, and the major spectroscopic constants, (R_e, ω_e, D_e), for all A_2 molecules (A = C–F) are listed in Table 1, along with the corresponding CCSD(T)/RCCSD(T)[34–36] and experimental values.[37,38] Note the overall excellent agreement between the vCASCI results and the CCSD(T)/RCCSD(T) results. This agreement supports the use of vCASCI calculations to calculate the potential energy curves for the A_2 molecules. The vCASCI results are also in good agreement with the experimental results, which provides a measure of the accuracy of the calculations. In particular, the errors of 2–4 kcal mol^{-1} in D_e suggests that $\Delta E_{DEC}(R)$ should be nearly quantitatively correct. These errors are primarily due to basis set limitations and the neglect of core–valence correlation effects. As these errors are only a few percent as judged by the errors in D_e, they are not expected to affect the conclusions drawn in the current study and, for the sake of simplicity, we decided to neglect them.

Table 1 Total energies (E_e at R_e) and equilibrium bond distances (R_e), fundamental frequencies (ω_e), and bond energies (D_e) for the A_2 molecules (A = C–F). Total energies (E_e) are in hartrees, bond distances (R_e) in Å, fundamental frequencies (ω_e) in cm^{-1}, and bond energies (D_e) in kcal mol^{-1}

	C_2	N_2	O_2	F_2
SCGVB				
E_e	−75.594679	−109.073564	−149.729913	−198.844910
R_e	1.244	1.096	1.200	1.467
ω_e	1843	2369	1579	698.8
D_e	112.6	171.4	68.6	16.6
vCASCI				
E_e	−75.794748	−109.392392	−150.147042	−199.324611
R_e	1.248	1.101	1.208	1.415
ω_e	1841	2350	1584	895.9
D_e	144.1	225.1	116.4	34.8
CCSD(T)				
E_e	−75.802143	−109.407243	−150.177985	−199.365736
R_e	1.246	1.100	1.208	1.413
ω_e	1854	2354	1601	921.4
D_e	143.6	224.1	118.0	37.8
Experimental[37,38]				
R_e	1.2425	1.09768	1.20752	1.41193
ω_e	1854.71	2358.57	1580.19	916.64
D_e	146.6	228.2	120.2	38.2

The changes in the spectroscopic constants resulting from the inclusion of dynamical electron correlation are plotted in Fig. 1. As expected, dynamical electron correlation has a major effect on the calculated dissociation energies increasing the predicted D_e's by 18.1 kcal mol^{-1} (F_2) to 53.6 kcal mol^{-1} (N_2). The increase in D_e is a measure of the difference in the dynamical electron correlation energy, $E_{DEC}(R)$, at $R = R_e$ and $R = 20.0$ Å ($\approx \infty$); see Table 2.

The changes in R_e and ω_e resulting from the inclusion of dynamical electron correlation are not related to the magnitude

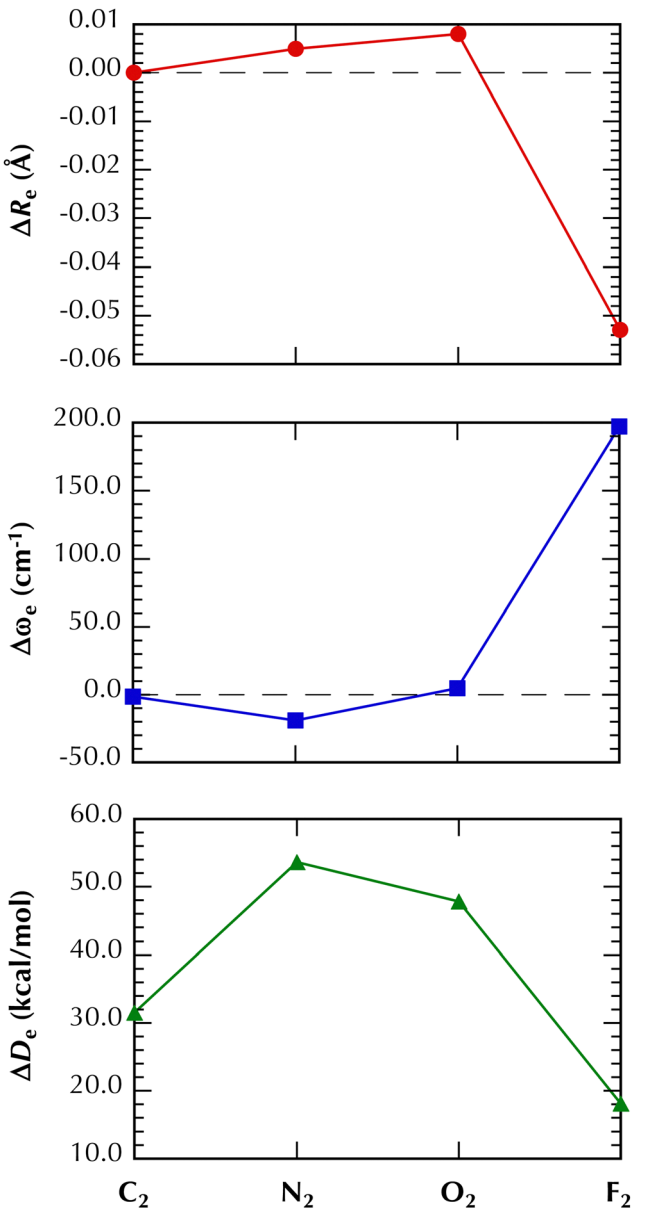

Fig. 1 Changes in the spectroscopic constants of C_2–F_2 resulting from inclusion of dynamical electron correlation, *e.g.*, $\Delta R_e = R_e$(vCASCI) − R_e(SCGVB).

Table 2 Total energies of the A_2 molecules (A = C–F) at the equilibrium internuclear distances (R_e) from the vCASCI calculations, total energies from SCGVB and vCASCI calculations R = 20.0 Å, and the differences in the dynamical electron correlation energies (E_{DEC}, ΔE_{DEC}). Total energies are in hartrees; energy differences are in kcal mol^{-1}

	C_2	N_2	O_2	F_2
$R = R_e$(vCASCI)				
E(SCGVB)	−75.594662	−109.073489	−149.729827	−198.843909
E_e(vCASCI)	−75.794748	−109.392392	−150.147042	−199.324611
$E_{DEC}(R_e)$	−125.56	−200.11	−261.81	−301.65
R = 20.0				
E(SCGVB)	−75.415205	−108.800450	−149.620647	−198.818418
vCASCI	−75.565114	−109.033689	−149.961517	−199.269201
$E_{DEC}(R$ = 20.0)	−94.07	−146.36	−213.90	−282.87
$\Delta E_{DEC}(R_e)$	−31.49	−53.75	−47.91	−18.78

of $\Delta E_{DCE}(R_e)$ but rather to changes in the shape of the $\Delta E_{DCE}(R)$ curve in the vicinity of R_e. In particular, the changes in R_e are related to the changes in the slope of $\Delta E_{DCE}(R)$ near R_e, while the changes in ω_e are related to the changes in the curvature of $\Delta E_{DCE}(R)$ near R_e. From Table 1 and Fig. 1, we find that:

• Inclusion of dynamical electron correlation has only a modest effect on the calculated R_e for C_2–O_2, with the resulting shifts ranging from +0.003 Å to +0.008 Å. However, it has a major effect on $R_e(F_2)$, decreasing R_e by 0.053 Å.

• Inclusion of dynamical electron correlation also has only a relatively modest effect on the calculated ω_e's for C_2–O_2: −1.4 cm^{-1} (C_2), −19.8 cm^{-1} (N_2) and +7.0 cm^{-1} (O_2). Again, the effect on ω_e of F_2 is far larger, +197.3 cm^{-1}.

The above results indicate that the changes in $\Delta E_{DCE}(R)$ near R_e are very different in F_2 than in C_2–O_2. This is surprising as it might have been thought that, as R decreases, the electrons in all four molecules would be forced into a smaller and smaller space, suggesting that the magnitude of the dynamical correlation energy would increase monotonically with decreasing R. This, in turn, would predict a decrease in R_e in all four molecules. However, this is not the case: R_e increases in C_2–O_2 and decreases only for F_2. This change in sign is a direct reflection of the changes in the slopes of the $\Delta E_{DCE}(R)$ curves near R_e—see the discussion of $\Delta E_{DEC}(\Delta R_e)$ in the third section. The large changes in all the spectroscopic constants for F_2 resulting from the inclusion of dynamical electron correlation is due to the repulsive interactions associated with the π lone pairs on the two fluorine atoms in this molecule. There are no π lone pairs in C_2 and N_2 and the three-electron interactions in the π_x and π_y systems in O_2 are attractive, not repulsive as they are in F_2. The large changes in the spectroscopic constants of F_2 is a direct result of the increasing importance of dynamical correlation of the electrons in the lone pairs of F_2 with decreasing R. Similar arguments rationalize the changes in ω_e. The irregular changes in (D_e, R_e, ω_e) are similar to the irregularities found in the AH and AF (A = C–F) series.[11]

Dynamical electron correlation in the C_2 molecule

Although we had no difficulty computing the SCGVB wavefunction for C_2 as a function of R, we found there were significant issues with the potential energy curves in the vCAS and vCASCI calculations. This is consistent with the findings of earlier researchers who found a strong interaction between the $X^1\Sigma_g^+$ and $B'^1\Sigma_g^+$ states in C_2 in the vicinity of R = 1.6 Å.[39–44] To address this issue, we included both states in state-averaged vCAS calculations. But the resulting potential energy curves still had irregularities. Finally, including three states in the state-averaged vCAS calculations resulted in stable and reasonable vCAS and vCASCI potential energy curves, see Fig. 2. This figure includes plots of the three potential energy curves obtained in this last set of calculations (the third curve corresponds to a $^1\Delta$ state). This figure also includes an inset of the difference between the energies of the $X^1\Sigma_g^+$ and $B'^1\Sigma_g^+$ states. The inset shows that the closest approach of the $X^1\Sigma_g^+$ and $B'^1\Sigma_g^+$ potential energy curves occurs at R = 1.59 Å and is only slightly greater than zero, in agreement with the earlier studies.

As large R, the magnitude of $\Delta E_{DEC}(R)$ increases with decreasing R as would be expected, but, as R continues to decrease the rate of decrease slows and then the magnitude of $\Delta E_{DEC}(R)$ begins to gradually decrease, yielding a minimum in the $\Delta E_{DEC}(R)$ curve; see Fig. 3. The minimum in the curve is at R = 1.82 Å. As will be shown later, this behavior is also observed for N_2 and O_2 with a slight hint of such behavior for F_2. From R = 1.82 Å to R = 1.59 Å, the magnitude of $\Delta E_{DEC}(R)$ steadily decreases, after which there is only a modest variation in

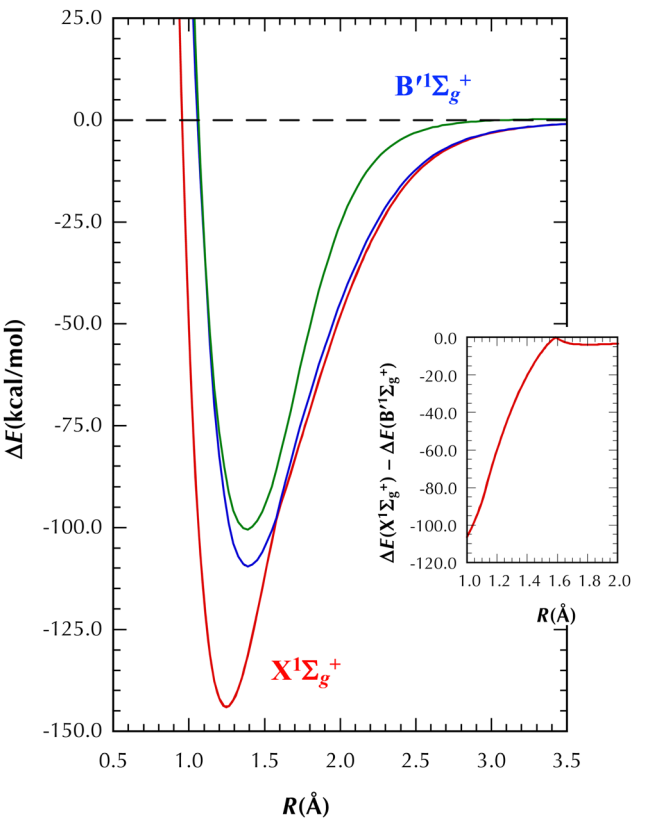

Fig. 2 The calculated (vCASCI) potential energy curves of C_2 for the three states included in the state-averaged vCAS calculations. The inset is the difference in energies of the $X^1\Sigma_g^+$ and $B'^1\Sigma_g^+$ states in kcal mol^{-1}. The point of closest approach of the potential energy curves for the $X^1\Sigma_g^+$ and $B'^1\Sigma_g^+$ states is at 1.59 Å.

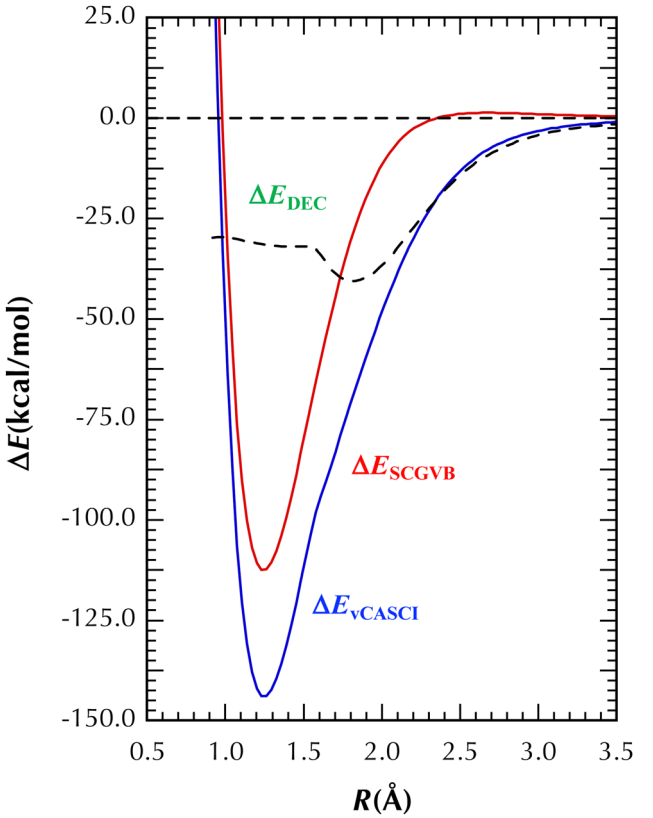

Fig. 3 The potential energy curves, ΔE_{SCGVB} and ΔE_{vCASCI}, for the $X^1\Sigma_g^+$ state of C_2 along with $\Delta E_{DEC}(R)$. The minima in the potential energy curves are at R_e = 1.244 Å (SCGVB) and 1.248 Å (vCASCI). The minimum in the $\Delta E_{DEC}(R)$ curve is at 1.82 Å. The visible bend in ΔE_{vCASCI} at R = 1.59 Å is due to the interaction between the $X^1\Sigma_g^+$ and $B'^1\Sigma_g^+$ states.

$\Delta E_{DEC}(R)$ with continuing decreases in R. Note that $\Delta E_{DEC}(R)$ is nearly flat in the vicinity of R_e, with $\Delta E_{DEC}(R_e)$ = −31.5 kcal mol^{-1}. Thus, despite the large increase in D_e due to dynamical electron correlation, the near constancy of $\Delta E_{DEC}(R)$ in the region around R_e results in only a minor shift in the calculated values of R_e and ω_e as observed in the last subsection.

But what accounts for the unusual behavior of $\Delta E_{DEC}(R)$ in C_2? First, what accounts for the minimum in $\Delta E_{DEC}(R)$ at R = 1.82 Å and, second, what is the underlying cause of the flattening of $\Delta E_{DEC}(R)$ for R less than 1.59 Å? Regarding the first question, we believe that it is highly unlikely that the minimum in $\Delta E_{DEC}(R)$ in C_2 is a result of the interaction between the $X^1\Sigma_g^+$ and $B'^1\Sigma_g^+$ states because we see the same behavior in N_2 and O_2. We will defer further discussion of this issue until the last section where we will examine the SCGVB wavefunction of N_2 in the vicinity of the minimum in $\Delta E_{DEC}(R)$. Regarding the flattening in $\Delta E_{DEC}(R)$, we note that the point at which $\Delta E_{DEC}(R)$ flattens with decreasing R is essentially the point of maximum interaction between the $X^1\Sigma_g^+$ and $B'^1\Sigma_g^+$ states of C_2, namely, R = 1.59 Å. However, there is little reason to assume that this interaction is responsible for the flattening of $\Delta E_{DEC}(R)$ for values of R much less that R = 1.59 Å since the gap between the two curves increases rapidly for R less than 1.59 Å (see the inset to Fig. 2). Thus, although the shape of $\Delta E_{DEC}(R)$ is influenced by the interaction between the $X^1\Sigma_g^+$ and $B'^1\Sigma_g^+$ states in the vicinity of R = 1.59 Å, it is unlikely that the $X^1\Sigma_g^+$–$B'^1\Sigma_g^+$ interaction is the cause of the flattening of $\Delta E_{DEC}(R)$ at much shorter values of R.

In prior SCGVB calculations on C_2[23,24] it was found that, unlike most molecules, two SCGVB configurations were required to properly describe the electronic structure of C_2:

1. The perfect pairing configuration, which couples the spins of the electrons in the doubly occupied $C_A2s'_+$ and $C_B2s'_-$ orbitals and the ($C_A2p\pi'_x$, $C_B2p\pi'_x$), ($C_A2p\pi'_y$, $C_B2p\pi'_y$), and ($C_A2s'_-$, $C_B2s'_+$) orbital pairs into singlets, and

2. The quasi-atomic configuration, which couples the spins of the electrons in the doubly occupied $C_A2s'_+$ and $C_B2s'_-$ orbitals into singlets with the spins of the electrons in the two remaining sets of orbitals, ($C_A2s'_-$, $C_A2p\pi'_x$, $C_A2p\pi'_y$) and ($C_B2s'_+$, $C_B2p\pi'_x$, $C_B2p\pi'_y$), each coupled into quartets with these two, three-electron quartet spin functions then being coupled to give an overall singlet state.

The second configuration was found to be the dominant SCGVB configuration around R_e. Thus, around R_e the spins of the electrons in six of the eight orbitals are high spin coupled in this configuration. Fermi correlation[45] between the electrons in these orbitals will moderate the magnitude of the dynamical electron correlation between the electrons in these orbitals and could well be responsible for the flattening of the $\Delta E_{DEC}(R)$ curve at short R.

We examined the total singlet and triplet spin couplings, $w_{\alpha\beta}(\varphi_{ai},\varphi_{aj})$ and $w_{\alpha\alpha}(\varphi_{ai},\varphi_{aj})$, for the various orbital pairs in the SCGVB wavefunction of C_2.[46] Although this analysis confirmed the unusual nature of the SCGVB wavefunction for this molecule, it did not provide a clear reason for the unusual behavior of the dynamical correlation energy, $\Delta E_{DEC}(R)$.

Dynamical electron correlation in the N_2–F_2 molecules

As would be expected the magnitude of E_{DEC} increases systematically from C_2 to F_2, reflecting the increase in the number of electrons in the valence orbitals in these molecules. This is illustrated in Table 2 and Fig. 4(a), which is a plot of $E_{DEC}(R)$ for the A_2 molecules. However, the magnitude of $E_{DEC}(R)$ is largely a reflection of the increase in the magnitude of $E_{DEC}(R = \infty)$ for the separated atoms; see Table 2. If we consider $\Delta E_{DEC}(R)$ or $\Delta E_{DEC}(\Delta R)$, the latter of which is plotted in Fig. 4(b), we find that for the A_2 molecules, the magnitude of $\Delta E_{DEC}(\Delta R = 0)$ increases in the sequence $N_2 > O_2 > C_2 > F_2$ (see also Table 2). Further, the gap between C_2 and N_2, 22.1 kcal mol^{-1}, is nearly four times the gap between N_2 and O_2, 5.8 kcal mol^{-1}, which is consistent with the unusual nature of the electronic structure of C_2 as discussed in the preceding subsection.

The plots in Fig. 4(b) show that the variation of ΔE_{DEC} with ΔR is clearly not monotonic. Given that the sizes of the orbitals involved in the bonding in the A_2 molecules steadily decrease from the carbon atom to the fluorine atom, at large R, the magnitude of $\Delta E_{DEC}(\Delta R)$ decreases steadily from C_2 to F_2 and the magnitude of $\Delta E_{DEC}(\Delta R)$ increases fastest with decreasing ΔR in this same sequence. The plot of $\log|\Delta E_{DEC}(R)|$ in Fig. 5

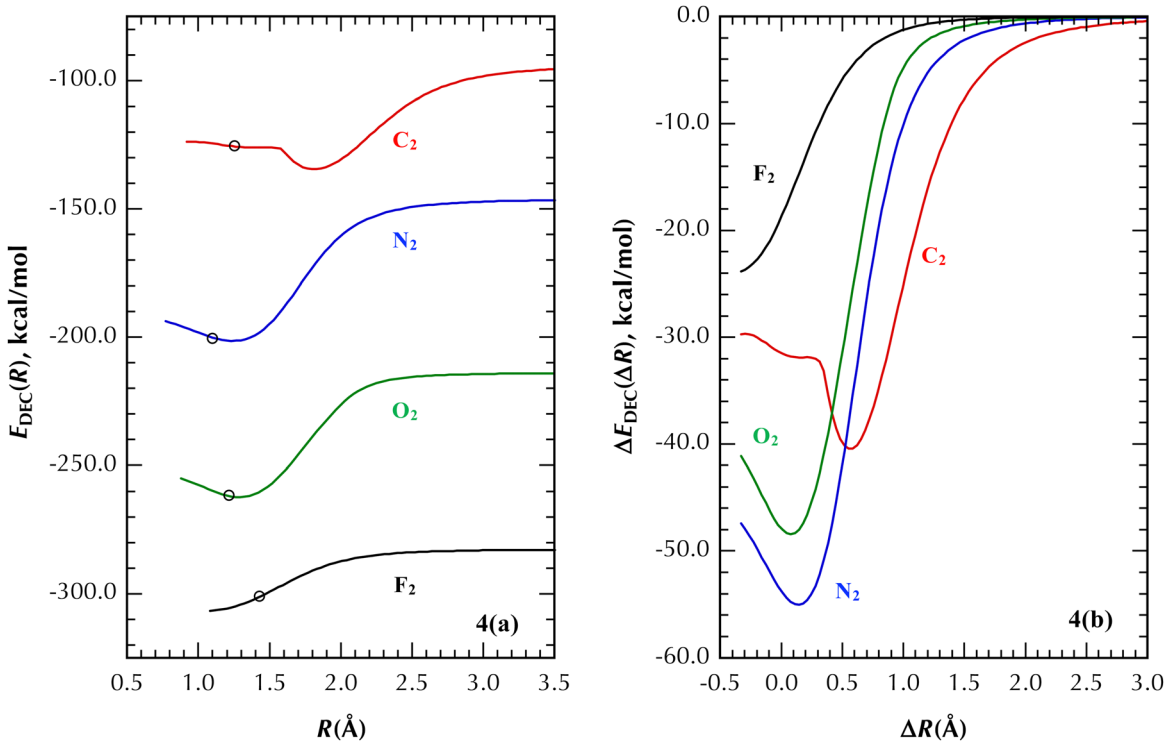

Fig. 4 (a) The total dynamical electron correlation energy, $E_{DEC}(R)$, for the ground states of C_2, N_2, O_2 and F_2, and (b) the dynamical electron correlation energy relative to that of the separated atoms (R = 20.0 Å) shifted by the calculated equilibrium internuclear distances, $\Delta E_{DEC}(\Delta R)$, where $\Delta R = R - R_e$. In Fig. 4(a) the circles on each curve are located at the calculated R_e for the given molecule. The minima in the $\Delta E_{DEC}(\Delta R)$ curves in (b) are at ΔR = 0.57 Å (C_2), 0.14 Å (N_2) and 0.08 Å (O_2).

reinforces this conclusion, where it is further seen that at large R, $\log|\Delta E_{DEC}(R)|$ increases nearly exponentially with decreasing R, although there is a slight positive curvature, especially for O_2. As ΔR continues to decrease, the behavior of $\Delta E_{DEC}(\Delta R)$ clearly fits a pattern except for that for C_2, which has a minimum as found in N_2 and O_2, but, as noted in the previous section, at ΔR = 0.34 Å (R = 1.59 Å), the $\Delta E_{DEC}(\Delta R)$ curve notably flattens, changing more modestly with further decreases in ΔR (R).

In Fig. 6, we plot $\Delta E_{DEC}(R)$ along with the calculated potential energy curves, $\Delta E_{vCASCI}(R)$, for N_2–F_2 (the corresponding plot for C_2 is given in Fig. 3). As can be seen, there are significant variations in $\Delta E_{DEC}(R)$ for all molecules within the bound region of the potential energy curves. Thus, dynamical electron correlation will have a significant effect on the properties of all four molecules, although, as shown for the spectroscopic constants, the details of the effect will be very different depending on the molecule and property of interest.

Analysis of the SCGVB wavefunction around the $\Delta E_{DEC}(\Delta R)$ minimum in N_2

The minima found in the $\Delta E_{DEC}(\Delta R)$ curves for C_2–O_2 in Fig. 4(b) are particularly puzzling. Why would the magnitude of the dynamical correlation energy decrease with further decreases in R, *i.e.*, as the electrons are crowded into an ever-smaller space. As can be seen, the minimum is deepest for N_2 then O_2 and finally C_2. Although the curve for F_2 does not show a minimum for the range of ΔR considered, there is a clear upward trend in $\Delta E_{DEC}(\Delta R)$ as short ΔR. So, the phenomenon seems to be universal for all four molecules, if not yet fully realized for F_2 for the range of ΔR considered.

The minima occur at ΔR (R) = 0.57 Å (1.82 Å) for C_2, 0.14 Å (1.24 Å) for N_2, and 0.08 Å (1.29 Å) for O_2. Although the minimum for C_2 is far from R_e, the minima for N_2 and O_2 are very close to R_e. To identify any possible correlation between these minima and changes in the SCGVB wavefunctions similar to the correlations found in our earlier studies,[11,12] we examined the SCGVB wavefunction for the N_2 molecule around the minimum. The SCGVB wavefunction is characterized by three quantities: (i) the geometry of the molecule, (ii) the SCGVB orbitals, and (iii) the spin function, *i.e.*, the $\{c_{S,k}\}$ in eqn (2). In addition, there are two other characteristics of the SCGVB wavefunction of interest: (iv) the approximate atomic orbital composition of the SCGVB orbitals[47,48] and (v) the overlap of the non-orthogonal SCGVB orbitals.

The SCGVB valence orbitals of N_2 are plotted in Fig. 7 in the region around the minimum in $\Delta E_{DEC}(R)$ at R = 1.24 Å. Although changes in the orbitals are visually evident as ΔR increases from ΔR = 0.94 Å to ΔR = 1.54 Å, *e.g.*, increases in the size of the $N_A2p\sigma'$ and $N_A2p\pi'_x$ bond orbitals and the increasing N_A2s character of the lone pair orbital, the changes appear to be smoothly monotonic. This conclusion is reinforced by the variations in the atomic orbital composition of the SCGVB orbitals in the top two panels in Fig. 8 (for definitions of the quantities in these figures, see ref. 46). In particular, we found that:

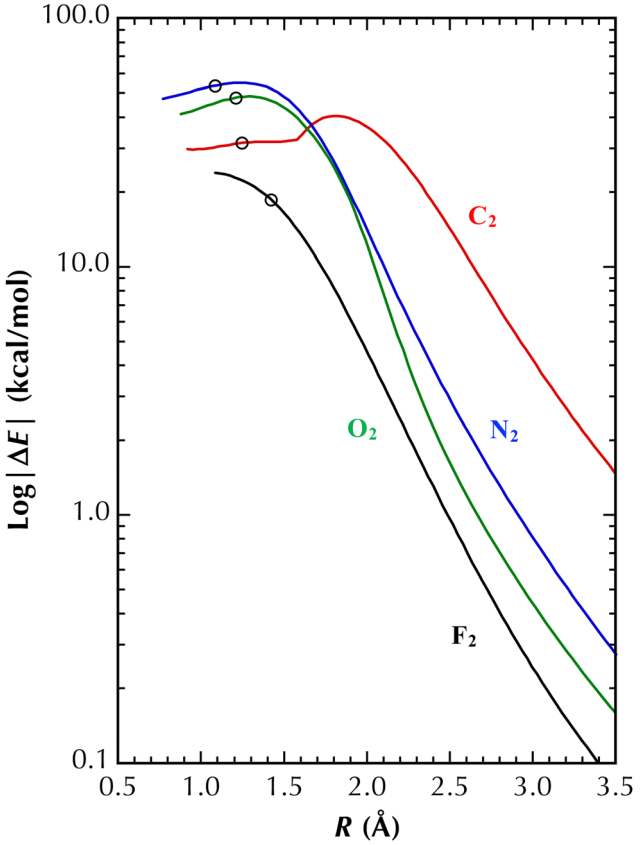

Fig. 5 Variation of $\log|\Delta E_{DEC}(R)|$ for the A_2 molecules. The circles are located at the calculated equilibrium internuclear distances, R_e, for each molecule.

• The N_A2s atomic orbital character of the $N_A2p\sigma'$ bond orbital, $P_{N_A2s}{}^2$, steadily decreases and the $N_A2p\sigma$ atomic orbital character, $P_{N_A2p\sigma}{}^2$, steadily increases as R increases. In addition, delocalization of the $N_A2p\sigma'$ orbital onto the N_B atom, as measured by $P_{N_B2s+N_B2p\sigma}{}^2$, decreases significantly as R increases. In short, the $N_A2p\sigma'$ bond orbital becomes progressively more $N_A2p\sigma$-like as R increases, but little else is evident.

• The N_A2s atomic orbital character of the N_A2s' lone pair orbital increases significantly with increasing R, while the $N_A2p\sigma$ atomic orbital character of the N_A2s' orbital decreases. Thus, the N_A2s' bond orbital becomes progressively more N_A2s-like as R increases. Note that this orbital is largely a hybrid atomic orbital for all R considered as shown by the fact that $P_{N_A2s+N_A2p\sigma}{}^2$ is close to unity throughout the region and $P_{N_B2s+N_B2p\sigma}{}^2$ is relatively small, especially for R greater than the minimum.

This analysis is consistent with the previous visual analysis of the SCGVB orbitals in Fig. 7 and offers no clear rationale for the minimum in $\Delta E_{DEC}(R)$ in N_2. Two other characteristics of the SCGVB wavefunction are plotted in Fig. 8: the overlap between the bond orbitals, $S(\varphi_{ai},\varphi_{aj})$, and the spin coupling coefficients, $\{c_{S,k}\}$. These quantities also change smoothly over the region of interest yielding no insight into the cause of the minimum in $\Delta E_{DEC}(R)$.

In summary, the above analysis of the changes in the SCGVB wavefunction for N_2 in the vicinity of the minimum in $\Delta E_{DEC}(R)$ provides no clear rationale for the minimum. Whatever is responsible for the minimum in $\Delta E_{DEC}(R)$ must be the result of more subtle changes in the electronic structure of the molecule. Perhaps it is an interplay between the localization of the bonding orbitals in the N_A–N_B region and the localization of the lone pair orbitals away from the N_A–N_B region as R decreases that leads to this behavior. Further exploration of this phenomenon is clearly warranted.

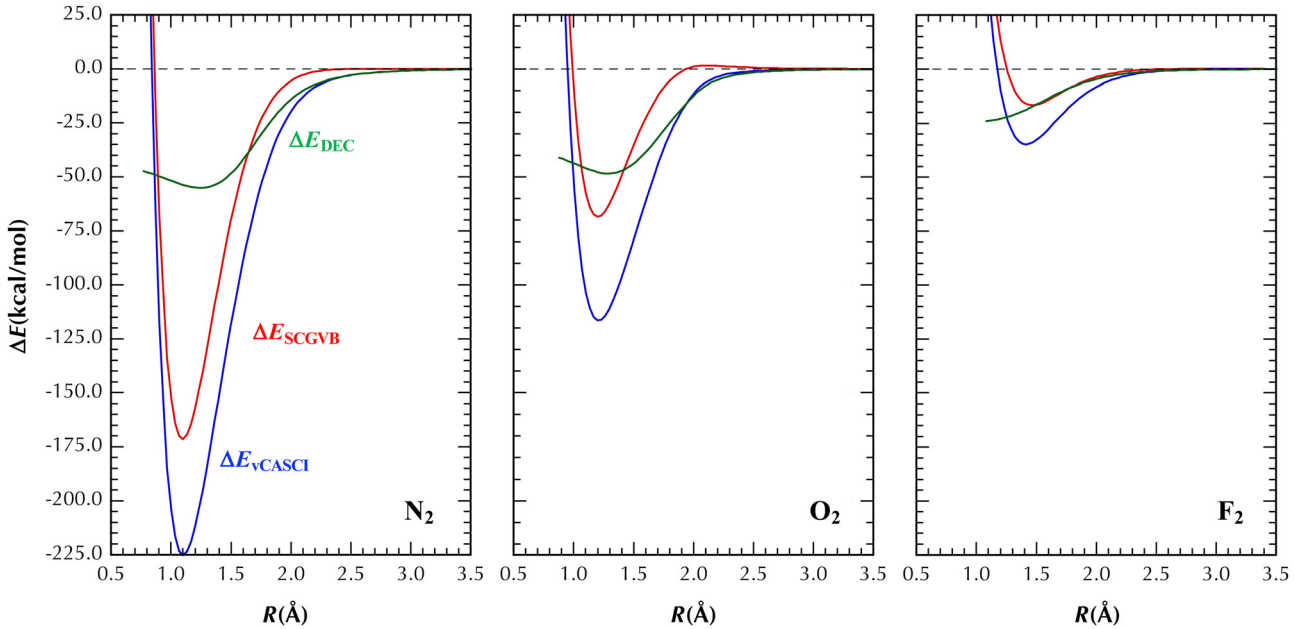

Fig. 6 Potential energy curves, ΔE_{SCGVB} and ΔE_{vCASCI}, for the ground states of N_2, O_2 and F_2 along with the changes in the dynamical correlation energies relative to that of the separated atoms, $\Delta E_{DEC}(R)$.

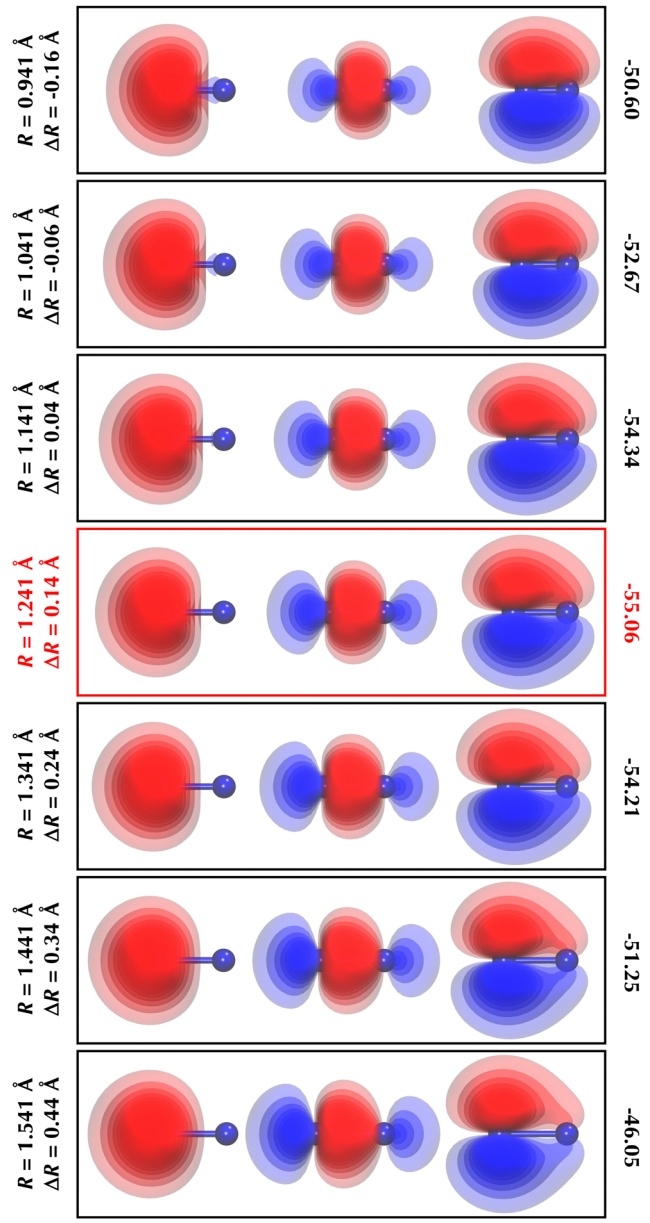

Fig. 7 Contour plots of the SCGVB valence orbitals, (N_A2s', $N_A2p\sigma'$, $N_A2p\pi'$), in the vicinity of the minimum in $\Delta E_{DEC}(R)$ for N_2. The internuclear distance, R and ΔR, is on the left and $\Delta E_{DEC}(R)$ is on the right. The minimum in $\Delta E_{DEC}(R)$ is at 1.24 Å (ΔR = 0.14 Å). Only the orbitals centered on atom N_A are shown; the orbitals on atom N_B are mirror images of those on atom N_A.

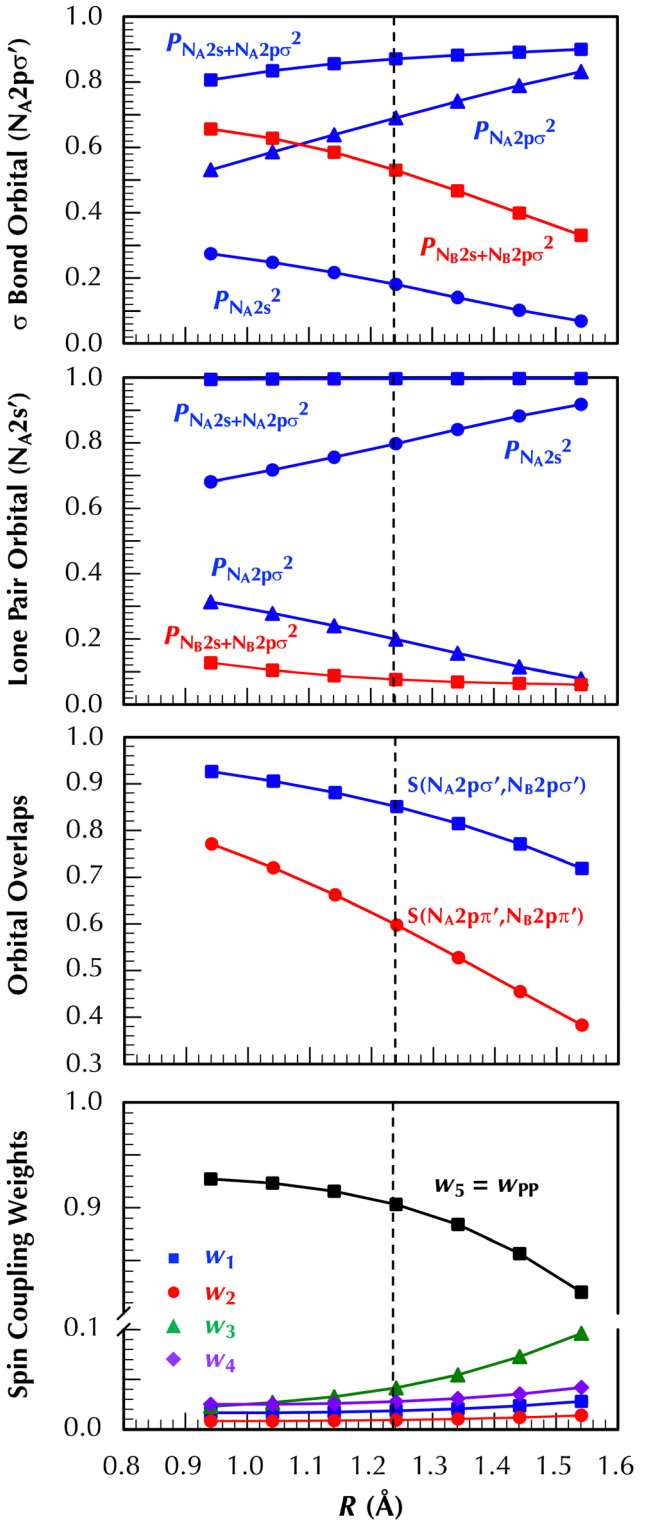

Fig. 8 Variation of selected characteristics of the SCGVB wavefunction in the vicinity of the minimum in $\Delta E_{DEC}(R)$ for N_2: atomic orbital analysis (top two plots), orbital overlaps (third plot) and spin-coupling weights (bottom plot). The dashed vertical line is drawn at the minimum (R = 1.24 Å).

Conclusions

In this article we examined the impact of dynamical electron correlation on the spectroscopic constants, (R_e, ω_e, D_e), and potential energy curves of the homonuclear diatomic A_2 molecules, (A = C–F). The current study is closely related to our previous study of the effect of dynamical electron correlation on the AH and AF molecules (A = B–F).[11,12] The dynamical correlation energy, $E_{DEC}(R)$, in all three studies was taken to be the difference in the energies obtained from vCASCI (vCAS + 1 + 2) and SCGVB calculations. Of particular interest is the correlation energy of the A_2 molecules relative to that of the separated atoms, $\Delta E_{DEC}(R)$, and the R_e-shifted value of $\Delta E_{DEC}(R)$, $\Delta E_{DEC}(\Delta R)$, with $\Delta R = R - R_e$ as the relative magnitudes of

the dynamical correlation effect is very different for the two latter cases.

This study led to four major findings and one subsidiary finding about the effect of dynamical electron correlation on the spectroscopic constants and potential energy curves of the A_2 molecules:

• Although the magnitude of $E_{DEC}(R)$ is largest for F_2 at $R = \infty$ and decreases as expected from F_2 to C_2, the magnitude of $\Delta E_{DEC}(R)$ does not follow this trend and, in fact, the trend changes as a function of R. For example, $\Delta E_{DEC}(R_e)$ decreases in the sequence $N_2 > O_2 > C_2 > F_2$. Thus, there is no correlation between the relative magnitudes of $E_{DEC}(R)$ and that of $\Delta E_{DEC}(R)$.

• At large R, the magnitude of $\Delta E_{DEC}(R)$ increases almost exponentially with decreasing R, but, as R continues to decrease, there are well-formed minima in $\Delta E_{DEC}(R)$ for C_2–O_2. The minima in these molecules are at R (ΔR) = 1.82 (0.57) Å (C_2), 1.24 (0.14) Å (N_2), and 1.29 (0.08) Å (O_2). Even the plot of $\Delta E_{DEC}(R)$ for F_2 shows a discernible upward trend at very short R, although there is no minimum in $\Delta E_{DEC}(R)$ for the range of R considered (the smallest value of which is already well up on the repulsive wall of the potential energy curve).

• The changes in $\Delta E_{DEC}(R)$ affect the potential energy curves and spectroscopic constants, (D_e, R_e, ω_e), of the A_2 molecules very differently, depending on the magnitude, slope, and curvature of $\Delta E_{DEC}(R)$ around R_e. The changes in the dissociation energy, D_e, are related to changes in the magnitude of $\Delta E_{DEC}(R)$ at R_e while the changes in the equilibrium internuclear distance, R_e, and fundamental frequency, ω_e, are related to changes in the slope and curvature of $\Delta E_{DEC}(R)$, respectively, around R_e.

■ The impact of dynamical electron correlation on the spectroscopic constants varies substantially: it has a major effect on D_e for all four molecules, with the increase in D_e varying from 18.1 kcal mol^{-1} for F_2 to 53.6 kcal mol^{-1} for N_2. The effect of dynamical electron correlation on R_e and ω_e is far less dramatic, except for F_2, where it decreases R_e by 0.053 Å and increases ω_e by 197.3 cm^{-1}. The latter is due to the dynamical correlation associated with the doubly occupied π systems in F_2.

The C_2 molecule is somewhat of an outlier in the A_2 series.

• Although $\Delta E_{DEC}(R)$ for C_2 increases approximately exponentially at large R as it does in the other A_2 molecules and $\Delta E_{DEC}(R)$ has a minimum as do the curves for N_2 and O_2, $\Delta E_{DEC}(R)$ varies only modestly for $R < 1.59$ Å. This value of R corresponds to the point of maximum interaction between the $X^1\Sigma_g^+$ and $B'^1\Sigma_g^+$ states in C_2. However, this interaction decreases rapidly for $R < 1.59$ Å and is likely not the cause of the flattening of the $\Delta E_{DEC}(R)$ curve for values of R significantly less than 1.59 Å. The flattening of $\Delta E_{DEC}(R)$ at short R may be due to the unusual nature of the electronic structure of the C_2 molecule, where the dominant SCGVB configuration couples the spins of six of the eight electrons in the SCGVB wavefunction into quartets, with Fermi correlation among these electrons decreasing the dynamical correlation energy.

The second finding, *i.e.*, the presence of minima in the $\Delta E_{DEC}(R)$ and $\Delta E_{DEC}(\Delta R)$ curves for C_2–O_2, is the most puzzling finding in this study. In previous studies of the effect of dynamical electron correlation on the potential energy curves of the AH and AF molecules, we were able to correlate the changes in $\Delta E_{DEC}(R)$ with changes in the nature of the SCGVB wavefunction (orbitals and/or spin coupling coefficients) for the AH and AF (A = B–F) molecules.[11,12] In the present case, a detailed analysis of the SCGVB wavefunction for N_2, which has the deepest minimum, revealed no clear reason for the presence of the minimum. Thus, more subtle aspects of the electronic wavefunction of these molecules must be at play. Further studies are clearly warranted.

Although this study along with our previous two studies[11,12] have led to a much improved understanding of dynamical electron correlation and its effect on molecular potential energy curves and spectroscopic constants of the diatomic molecules studied, it also shows that we still have much to learn about the basic nature of dynamical electron correlation and its effects on molecular properties and molecular processes. Given that the SCGVB wavefunction describes non-dynamical electron correlation and only non-dynamical electron correlation, we can use the approach described here to examine the impact of dynamical electron correlation on other molecular properties as well as molecular processes such as chemical reactions.

Data availability

The data supporting this article have been included as part of the ESI.†

Conflicts of interest

There are no conflicts of interest to declare.

Acknowledgements

This research was supported by the Center for Scalable Predictive methods for Excitations and Correlated phenomena (SPEC), which is funded by the U.S. Department of Energy, Office of Science, Basic Energy Sciences, Chemical Sciences, Geosciences and Biosciences Division as part of the Computational Chemical Sciences (CCS) program under FWP 70942 at Pacific Northwest National Laboratory (PNNL), a multiprogram national laboratory operated for DOE by Battelle. We wish to thank Professor David L. Cooper for assistance with the SCGVB(n,m) calculations on O_2.

References

1 P.-O. Löwdin, Correlation problem in many-electron quantum mechanics. View of different approaches and discussion of some current ideas, *Adv. Chem. Phys.*, 1958, **2**, 207–322.
2 O. Sinanoğlu, Many-electron theory of atoms, molecules and their interaction, *Adv. Chem. Phys.*, 1964, **6**, 315–412.

3 J. Linderberg and H. Shull, Electronic correlation energy in 3- and 4-electron atoms, *J. Mol. Spectrosc.*, 1960, **5**, 1–16.
4 E. Clementi and A. Veillard, Correlation energy in atomic systems. IV. Degeneracy effects, *J. Chem. Phys.*, 1966, **44**, 3050–3053.
5 C. A. Coulson and I. Fischer, XXXIV. Notes on the molecular orbital treatment of the hydrogen molecule, *Philos. Mag.*, 1949, **40**, 386–393.
6 T. Kato, On the eigenfunctions of many-particle systems in quantum mechanics, *Commun. Pure Appl. Math.*, 1957, **10**, 151–177.
7 R. T. Pack and W. Byers-Brown, Cusp conditions for molecular wavefunctions, *J. Chem. Phys.*, 1966, **45**, 556–559.
8 T. H. Dunning, Jr., L. T. Xu, D. L. Cooper and P. B. Karadakov, Spin-Coupled generalized valence bond theory: New perspectives on the electronic structure of molecules and chemical bonds, *J. Phys. Chem. A*, 2021, **125**, 2021–2050 and references therein.
9 E. Ramos-Cordoba, P. Salvador and E. Matito, Separation of dynamical and nondynamical correlation, *Phys. Chem. Chem. Phys.*, 2016, **18**, 24015–24023.
10 C. L. Benavides-Riveros, N. N. Lathiotakis and M. A. L. Marques, Towards a formal definition of static and dynamic electron correlations, *Phys. Chem. Chem. Phys.*, 2017, **19**, 12655–12664.
11 L. T. Xu and T. H. Dunning, Jr., Dynamical electron correlation and the chemical bond. I. Covalent bonds in AH and AF (A = B–F), *J. Chem. Phys.*, 2022, **157**, 014107.
12 T. H. Dunning, Jr. and L. T. Xu, Dynamical electron correlation and the chemical bond. II. Recoupled pair bonds in the $a^4\Sigma^-$ states of CH and CF, *J. Chem. Phys.*, 2022, **157**, 084124.
13 T. H. Dunning, Jr., L. T. Xu and T. Y. Takeshita, Fundamental aspects of recoupled pair bonds. I. recoupled pair bonds in carbon and sulfur monofluoride, *J. Chem. Phys.*, 2015, **142**, 034113.
14 D. K. W. Mok, R. Neumann and N. C. Handy, Dynamical and nondynamical correlation, *J. Phys. Chem.*, 1966, **100**, 6225–6230.
15 B. O. Roos, The complete active space self-consistent field method and its applications in electronic structure calculations, *Adv. Chem. Phys.*, 1987, **69**, 399–445.
16 J. S. Sears and C. D. Sherrill, On the choice of reference in multi-reference electronic structure theory: minimal references for bond breaking, *Mol. Phys.*, 2005, **103**, 803–814.
17 R. C. Ladner and W. A. Goddard, III, Improved Quantum Theory of Many-Electron Systems. V. The Spin-coupling Optimized GI Method, *J. Chem. Phys.*, 1969, **51**, 1073–1087.
18 J. Gerratt, D. L. Cooper, P. B. Karadakov and M. Raimondi, Modern Valence Bond Theory, *Chem. Soc. Rev.*, 1997, 87–100.
19 T. H. Dunning, Jr., L. T. Xu, T. Y. Takeshita and B. A. Lindquist, Insights into the Electronic Structure of Molecules from Generalized Valence Bond Theory, *J. Phys. Chem. A*, 2016, **120**, 1763–1778.
20 S. Wilson, On the wave function of Coulson and Fischer: A third way in quantum chemistry, *Prog. Theor. Chem. Phys.*, 2009, **19**, 269–294.
21 R. Pauncz, *Spin Eigenfunctions, Construction and Use*, Springer US, Boston, 1979; R. Pauncz, *The Construction of Spin Eigenfunctions, An Exercise Book*, Kluwer Academic/Plenum Publishers: New York, 2000.
22 E. Clementi and A. Veillard, Correlation energy in atomic systems. IV. Degeneracy effects, *J. Chem. Phys.*, 1966, **44**, 3050–3053.
23 L. T. Xu and T. H. Dunning, Jr., Insights into the perplexing nature of the bonding in C_2 from generalized valence bond calculations, *J. Chem. Theory Comput.*, 2014, **10**, 195–201.
24 D. L. Cooper, F. E. Penotti and R. Ponec, Why is the bond multiplicity in C_2 so elusive?, *Comput. Theoret. Chem.*, 2015, **1053**, 189–194.
25 P. B. Karadakov, D. L. Cooper and B. J. Duke, Spin-Coupled Theory for 'N Electrons in M Orbitals' Active Spaces, *J. Phys. Chem. A*, 2012, **116**, 7238–7244.
26 H.-J. Werner and P. J. Knowles, An efficient internally contracted multiconfiguration-reference configuration interaction method, *J. Chem. Phys.*, 1988, **89**, 5803–5814.
27 L. T. Xu and T. H. Dunning, Jr., A cautionary tale: Problems in the valence-CASSCF description of the ground state $(X^1\Sigma^+)$ of BF, *J. Chem. Phys.*, 2020, **153**, 114113.
28 T. H. Dunning, Jr., Gaussian basis sets for use in correlated calculations. I. Atoms boron through neon and hydrogen, *J. Chem. Phys.*, 1989, **90**, 1007–1023.
29 R. A. Kendall, T. H. Dunning, Jr. and R. J. Harrison, Electron affinities of the first-row atoms revisited. Systematic basis sets and wave functions, *J. Chem. Phys.*, 1992, **96**, 6796–6806.
30 H.-J. Werner, P. J. Knowles, R. D. Amos, A. Bernhardsson, A. Berning, P. Celani, D. L. Cooper, M. J. O. Deegan, A. J. Dobbyn and F. Eckert, *et al.*, *Molpro, version 2010.1, a package of ab initio programs*, see http://www.molpro.net.
31 H.-J. Werner, P. J. Knowles, G. Knizia, F. R. Manby and M. Schütz, M. Molpro: A General-Purpose Quantum Chemistry Program Package, *WIREs Comput. Mol. Sci.*, 2011, **2**, 242–253.
32 T. Thorsteinsson, D. L. Cooper, J. Gerratt, P. Karadakov and M. Raimondi, Modern Valence Bond Representations of CASSCF Wavefunctions, *Theor. Chim. Acta*, 1996, **93**, 343–366.
33 D. L. Cooper, T. Thorsteinsson and J. Gerratt, Fully Variational Optimization of Modern VB Wave Functions Using the CASVB Strategy, *Int. J. Quantum Chem.*, 1997, **65**, 439–451.
34 G. D. Purvis III and R. J. Bartlett, A full coupled-cluster singles and doubles model: The inclusion of disconnected triples, *J. Chem. Phys.*, 1982, **76**, 1910–1918.
35 K. Raghavachari, G. W. Trucks, J. A. Pople and M. Head-Gordon, A fifth-order perturbation comparison of electron correlation theories, *Chem. Phys. Lett.*, 1989, **157**, 479–483.
36 P. J. Knowles, C. Hampel and H.-J. Werner, Coupled cluster theory for high spin, open shell reference wave functions, *J. Chem. Phys.*, 1993, **99**, 5219–5227.
37 NIST Chemistry WebBook (Standard Reference Database Number 69), Constants of Diatomic Molecules; **https://webbook.nist.gov/chemistry/**; accessed on October 1, 2023.
38 B. Ruscic, D. Feller and K. A. Peterson, Active thermochemical tables: Dissociation energies of several homonuclear

first-row diatomics and related thermochemical values, *Theor. Chem. Acc.*, 2014, **133**, 1415.

39 M. Boggio-Pasqua, A. I. Voronin, Ph Halvick and J.-C. Rayez, Analytical representations of high level ab initio potential energy curves of the C2 molecule, *J. Mol. Struct.: THEOCHEM*, 2000, **531**, 159–167.

40 C. D. Sherrill and P. Piecuch, The $X^1\Sigma_g^+$, $B^1\Delta_g$, and $B'^1\Sigma_g^+$ states of C_2: A comparison of renormalized coupled-cluster and multireference methods with full configuration interaction benchmarks, *J. Chem. Phys.*, 2005, **122**, 124104.

41 A. J. C. Varandas, A simple, yet reliable, direct diabatization scheme. The $^1\Sigma_g^+$ states of C2, *Chem. Phys. Lett.*, 2009, **471**, 315–321.

42 X.-N. Zhang, D.-H. Shi, J.-F. Sun and Z.-L. Zhu, MRCI study of spectroscopic and molecular properties of $X^1\Sigma_g^+$ and $A^1\Pi_u$ electronic states of the C_2 radical, *Chin. Phys. B*, 2011, **20**, 043105.

43 C. Angeli, R. Cimiraglia and M. Pastore, A comparison of various approaches in internally contracted multireference configuration interaction: the carbon dimer as a test case, *Mol. Phys.*, 2012, **110**, 2963–2968.

44 J. S. Boschen, D. Theis, K. Ruedenberg and T. Windus, Accurate ab initio potential energy curves and spectroscopic properties of the four lowest singlet states of C_2, *Theor. Chem. Acc.*, 2014, **133**, 47–58.

45 D. P. Tew, W. Klopper and T. Helgaker, Electron correlation: The many-body problem at the heart of chemistry, *J. Comput. Chem.*, 2007, **28**, 1307–1320.

46 T. H. Dunning, Jr., D. L. Cooper, L. T. Xu and P. B. Karadakov, Spin-coupled generalized valence bond theory: An appealing orbital theory of the electronic structure of atoms and molecules, *Comprehensive Computational Chemistry*, Elsevier Inc., 2022, vol. 1, pp. 354–402.

47 L. T. Xu and T. H. Dunning, Jr., Orbital hybridization in modern valence bond wave functions: Methane, ethylene, and acetylene, *J. Phys. Chem. A*, 2020, **124**, 204–214.

48 L. T. Xu and T. H. Dunning, Jr., Correction to ''Orbital hybridization in modern valence bond wave functions: Methane, ethylene, and acetylene'', *J. Phys. Chem. A*, 2021, **125**, 9026.

